

# Investigation of the mobility of polybutadienes: 2. Fluorescence anisotropy decay of rod-like rigid probes

Mamadou Fofana, Valérie Veissier, Jean Louis Viovy and Lucien Monnerie\*

Laboratoire de Physico-Chimie Structurale et Macromoléculaire, (LA CNRS 278), ESPCI, 10 rue Vauquelin, 75231 Paris Cedex 05, France

(Received 19 May 1988; revised 4 July 1988; accepted 7 July 1988)

The dynamics of a series of polybutadienes with molecular weights 500, 1000, 2500 and 410 000 are studied using the fluorescence anisotropy decay of rod-like diphenylhexatriene and diphenyloctatetraene probes embedded in the polymer melt. The motion is shown to be viscous rotational diffusion, with slipping boundary conditions. The evolution of the correlation times with the molecular weight is in agreement with the Fox-Flory expression. The evolution as a function of the temperature is interpreted in terms of the WLF equation. A qualitative consistency between excimer fluorescence, fluorescence anisotropy decay, viscosity measurements and viscoelasticity is obtained. The probe factor for diphenylhexatriene is 1 in all polymers in the series, indicating that this probe is larger than the elementary kinetic unit of polybutadiene.

(Keywords: polybutadienes; fluorescence anisotropy decay; probes)

## INTRODUCTION

In the previous paper of this series<sup>1</sup>, the excimer formation of meso-2,4-di(*N*-carbazolyl)pentane was used to probe the dynamics of polybutadiene above its glass transition temperature. We pursue this study of polybutadiene (PB) using fluorescence anisotropy decay (f.a.d.) of rigid rod-like probes, diphenylhexatriene (DPH) and diphenyloctatetraene (DPO), in PB matrices of different molecular weight. This technique provides direct access to the orientation autocorrelation function. It allows a rather unambiguous understanding of the nature of the motions.

## EXPERIMENTAL

### Materials

Four polybutadiene matrices were used for this study. Two samples, PB500 and PB1000, have been described in the first paper of the series<sup>1</sup>. In addition we studied two samples with a high molecular weight. One with molecular weight about 2500, purchased from Polyscience, was used without further purification. A high-molecular-weight polybutadiene (PBh) was provided by la Manufacture des Pneumatiques Michelin. It was purified for 24 h by continuous extraction with distilled acetone, using Soxhlet glassware. The characteristics of the different PB samples are given in Table 1.

We used two types of f.a.d. probes: diphenylhexatriene (DPH) and diphenyloctatetraene (DPO). These molecules are privileged f.a.d. probes for several reasons: they are rigid with a rather simple geometry, and have a high quantum yield and a high fundamental anisotropy.

In particular, DPH has often been used in dynamics in biological systems<sup>2</sup>. These molecules (scintillator grade) were purchased from EGA, and used without further purification.

### Sample preparation

Samples with an optical density  $\leq 0.1$  (for 10 mm optical path) were prepared in order to avoid reabsorption. The low- $M_w$  samples ( $M_w \leq 2500$ ) have been prepared in standard Suprasil 10  $\times$  10 mm fluorescence cells, by direct dissolution of the fluorescence dye. Films 1 mm thick of PBh containing dispersed probes were cast from a solution of PBh and dye in chloroform. Complete removal of the solvent was achieved by gentle heating under vacuum. Then the films were moulded in special-purpose quartz cells<sup>3</sup>, and the stress induced by moulding was relaxed by further stoving under the same conditions.

### Principle of the experiments

The vertically and horizontally polarized fluorescence decays (resp.  $I_V$  and  $I_H$ ) following a vertically polarized excitation pulse are recorded alternately. The experimental anisotropy  $r_{\text{exp}}(t)$ , obtained as:

$$r_{\text{exp}}(t) = \frac{I_V(t) - gI_H(t)}{I_V(t) + 2gI_H(t)} \quad (1)$$

is then compared with a 'reconvoluted' anisotropy:

$$r_{\text{conv}}(t) = \frac{r(t)*F(t)}{I_V(t) + 2gI_H(t)} \quad (2)$$

using a non-linear least-squares iterative reconvolution algorithm<sup>4</sup>. In relation (2),  $F(t)$  represents the excitation pulse (recorded at emission wavelength), \* is the

\* To whom correspondence should be addressed

**Table 1** Characteristics and WLF parameters of the different polybutadienes examined

Symbol	$M_w$	$M_n$	Content (%)			$T_g$ (d.s.c.) (K)	From viscosity			From f.a.d.			$\tau_0$ $\times 10^3$ (ns)		
			cis	trans	vinyl		$T_\infty$ (K)	$C_1 C_2$	$C_1$	$C_2$	$T_\infty$ (K)	$C_1 C_2$		$C_1$	$C_2$
PB500	500	435	19	56	24	157	123 <sup>a</sup>	453 <sup>a</sup>	13.3 <sup>a</sup>	34 <sup>a</sup>	124 <sup>b</sup>	481 <sup>b</sup>	15 <sup>b</sup>	32 <sup>b</sup>	2.2 <sup>c</sup>
PB1000	1000	830	25	59	15	167	125 <sup>a</sup>	548 <sup>a</sup>	13.1 <sup>a</sup>	42 <sup>a</sup>	108 <sup>b</sup>	648 <sup>b</sup>	11 <sup>b</sup>	59 <sup>b</sup>	1.2 <sup>c</sup>
PB2500	2500	2170	37	56	8	172					107 <sup>b</sup>	660 <sup>b</sup>	10.1 <sup>b</sup>	65 <sup>b</sup>	
PBh	$4.1 \times 10^5$	$1.7 \times 10^5$	37	51	12	176					104 <sup>b</sup>	712 <sup>b</sup>	9.9 <sup>b</sup>	72 <sup>b</sup>	1.14 <sup>c</sup>
none			43	50	7	172	112 <sup>d</sup>	667 <sup>d</sup>	11.2 <sup>d</sup>	60 <sup>d</sup>					
none			96	2	2	161	101 <sup>d</sup>	678 <sup>d</sup>	11.3 <sup>d</sup>	60 <sup>d</sup>					
none			7	2	91	261	226 <sup>d</sup>	444 <sup>d</sup>	12.7 <sup>d</sup>	35 <sup>d</sup>					

<sup>a</sup>From viscosity, ref. 1

<sup>b</sup>From f.a.d., this study

<sup>c</sup>Combining viscosity from ref. 1 and f.a.d.

<sup>d</sup>From ref. 29

convolution symbol,  $g$  is a normalization factor (independently calibrated using quinine sulphate), and  $r(t)$  is the anisotropy

$$r(t) = r_0 P_2(t) \quad (3)$$

$r_0$  is the fundamental anisotropy, and  $P_2(t)$  is the second-order orientational autocorrelation function (OACF).

#### Apparatus

Experiments were performed using a f.a.d. apparatus using synchrotron radiation as the exciting source<sup>5</sup> (Cyclosynchrotron LURE-ACO, Orsay, France), operating in a single-photon-counting mode. The excitation wavelength (375 and 390 nm for DPH and DPO, respectively) was selected using a double holographic grating monochromator. The emission (448 and 500 nm respectively) was selected using a combination of Kodak band filters with narrow interferential filters (MTO). In addition, a few experiments were performed using a conventional flashlamp excitation ( $\lambda = 358$  nm) which provides a less accurate sampling of the OACF, but gives access to longer decay times because of a lower repetition rate. This apparatus was described elsewhere<sup>6</sup>. All data were treated on a NAS 9080 computer (CNRS-CIRCE, Orsay).

## PROBE DYNAMICS

### Decay of total intensity

We first performed a rather detailed investigation of the dynamics of DPH in PBh. In our experiments the total fluorescence intensity decay of DPH is correctly fitted by a single exponential, in agreement with a strong dominance of  $S_1 \rightarrow S_0$  fluorescence as already observed in various solvents<sup>2,7,8</sup>. It is worth quoting that other authors argued in favour of the presence of a second exponential with a smaller lifetime, and an integrated amplitude up to 15% of the integrated emission in polar solvents<sup>9</sup>. The question of this short-time exponential is still controversial, and it is bound to remain so to some extent, because many experimental artefacts such as pulse shape drift, stray light, radiofrequencies, photo-multiplier colour effect<sup>10</sup> or data quantization<sup>11</sup> are able to induce an apparent spurious component (or to hide an actual one) in the domain corresponding to the excitation pulse. In most cases, however, the reported integrated intensities are close to 1–2%<sup>12</sup>. The decays we

obtained in PBh for DPH and DPO also contain a weak short-time component (Tables 2 and 3) representing about 2% of total intensity for DPH, and 3% for DPO (with the exception of DPO at 335.4 K, which is probably artefactual). Since we are interested in polarization measurements, which involve other experimental uncertainties, and a signal-to-noise ratio much poorer than that of lifetime measurements, this component should not seriously affect our results. Moreover the correlation times we measure are generally larger than  $\theta_1$ . This also contributes to limit the influence of this component on the measured correlation times. Therefore, we assume in the following a simple  $S_1 \rightarrow S_0$  transition scheme for fluorescence, without changes of conformation, and we ignore possible more complicated schemes.

### Oriental autocorrelation function

Previous studies of the f.a.d. of this probe indicated that the OACF is close to a single exponential in simple viscous liquids<sup>13</sup>, in agreement with the prediction of viscous rotational diffusion of a spherical top (or rigid rod). It is worth noting, however, that other studies revealed a weak short-time component, attributed to a non-zero angle between the transition moment and the first hydrodynamic principal axis<sup>12</sup>. An angle of 15° at

**Table 2** Bi-exponential fit to the total fluorescence intensity decay of DPH in PBh

$T$ (K)	$a_1$	$\theta_1$	$a_2$	$\theta_2$	$a_2\theta_2/(a_1\theta_1 + a_2\theta_2)$	$\chi^2$
315.6	0.955	7.36	0.045	2.87	0.018	6.01
304.5	0.958	7.26	0.042	2.677	0.016	6.00
293.9	0.945	7.05	0.093	1.536	0.021	22.4
280.8	0.945	7.05	0.055	2.213	0.018	11.7
269.5	0.785	6.91	0.215	0.748	0.029	24.9

**Table 3** Bi-exponential fit to the total fluorescence intensity decay of DPO in PBh

$T$ (K)	$a_1$	$\theta_1$	$a_2$	$\theta_2$	$a_2\theta_2/(a_1\theta_1 + a_2\theta_2)$	$\chi^2$
335.4	0.815	6.49	0.185	2.40	0.078	7.69
315.6	0.898	6.61	0.102	2.31	0.038	7.69
304.3	0.927	6.73	0.073	2.88	0.033	7.92
293.8	0.843	6.87	0.157	1.29	0.034	50.9
281.2	0.914	7.07	0.086	1.75	0.023	17.9
269.2	0.948	7.30	0.052	3.18	0.023	10.8

most is predicted by the theory<sup>2</sup>, which should lead at most to a few per cent deviation from mono-exponential behaviour. Of course, the difficulty of extracting a weak short-time component noticed in the case of lifetime measurements is even more drastic in the case of anisotropy. Much stronger deviations from a mono-exponential *OACF* have been reported in some more complicated environments encountered in biological systems<sup>2,12,13</sup>. A typical case is membranes in which an orientational coupling, which tends to align the probe perpendicular to the membrane plane, leads to a non-zero anisotropy at infinite time. In the case of polymers, the correlation time of various rigid probes, including DPH and DPO, has been studied as a function of temperature, but, to our knowledge, no detailed study of the shape of the *OACF* has been performed.

Using depolarized Rayleigh scattering, Ouano and Pecora studied the reorientation of chlorobenzene (CB) in poly(methyl methacrylate) (PMMA) above and below the glass transition<sup>14</sup>. They observed a marked non-exponential character of the orientational multimolecular correlation function with two widely separated correlation times (nanosecond and picosecond range, respectively). This non-exponential character was attributed to a 'cage effect' formally very similar to the model of bounded rotation developed by Kinoshita<sup>15</sup> and successfully applied to biological membranes<sup>2</sup>, or to the presence of two distinct slowly exchanging environments for CB probes in PMMA<sup>15</sup>. The multimolecular orientational correlation functions observed in depolarized Rayleigh scattering are not as easily related with molecular motions as the *OACF*. It thus appeared rather interesting to check the generality of this observation, and to study whether or not the viscoelastic nature of PBh would induce on the *OACF* of DPH and DPO a deviation from the mono-exponential character observed in simple liquids. A partial answer to this question is contained in Tables 4 and 5, in which the f.a.d. of DPH and DPO at different temperatures has been fitted using three expressions for the *OACF*:

$$\begin{aligned} \text{1E: } r(t) &= r_0 \exp(-t/\tau) \\ \text{K: } r(t) &= r_1 \exp(-t/\tau) + r_{\text{inf}} \\ \text{2E: } r(t) &= r_1 \exp(-t/\tau_1) + r_2 \exp(-t/\tau_2) \end{aligned}$$

The first one (denoted '1E') is a single-exponential, corresponding to isotropic rotational diffusion. The second expression ('K') corresponds to rotational

**Table 4** Best fits to the f.a.d. of DPH in PBh

Model	Parameters	T (K)				
		315.6	304.5	293.9	280.8	269.5
1E	$a$	0.329	0.319	0.326	0.323	0.329
	$\tau(\text{ns})$	2.47	3.85	6.42	11.8	22.2
	$\chi^2$	1.63	1.52	1.78	3.45	2.03
K	$a_1$	0.322	0.319	0.321	0.323	0.308
	$\tau_1(\text{ns})$	2.45	3.82	6.09	11.76	19.81
	$a_2$	0.001	0.001	0.006	0.001	0.022
	$\chi^2$	1.60	1.32	1.40	3.44	1.99
2E	$a_1$	0.319	0.268	0.289	0.316	0.308
	$\tau_1(\text{ns})$	2.40	3.41	5.61	11.63	19.46
	$a_2$	0.005	0.005	0.004	0.008	0.023
	$\tau_2(\text{ns})$	5.0	6.4	15.8	22.9	1600
	$\chi^2$	1.49	1.32	1.40	3.44	1.99

**Table 5** Best fits to the f.a.d. of DPO in PBh

Model	Parameters	T (K)					
		335.4	315.6	304.3	293.8	281.2	269.3
1E	$a$	0.325	0.334	0.342	0.353	0.365	0.343
	$\tau(\text{ns})$	1.88	3.99	6.38	11.9	23.5	42.1
	$\chi^2$	4.61	2.45	1.84	4.89	3.03	4.22
K	$a_1$	0.324	0.328	0.333	0.318	0.304	0.311
	$\tau_1(\text{ns})$	1.66	3.60	5.78	9.18	17.2	36.7
	$a_2$	0.010	0.011	0.013	0.043	0.065	0.034
	$\chi^2$	3.17	1.64	1.22	2.06	2.20	4.16
2E	$a_1$	0.324	0.323	0.298	0.291	0.195	0.303
	$\tau_1(\text{ns})$	1.66	3.52	5.50	8.49	13.18	35.7
	$a_2$	0.011	0.017	0.017	0.071	0.174	0.041
	$\tau_2(\text{ns})$	6000	36	18	65	55	1500
	$\chi^2$	3.20	1.57	1.08	2.03	2.18	4.16

diffusion in a cone<sup>15</sup>. Finally, a bi-exponential expression which can reflect various types of anisotropic rotations<sup>16</sup> has been employed. It is worth noting that this expression contains four adjustable parameters, which makes it a very versatile curve-fitting expression for f.a.d. As expected, it provides the best values of  $\chi^2$  in all cases (fluctuations in the third figure are associated in uncertainties in the localization of the minimum). In all cases the fit reveals a strong exponential, with a correlation time regularly increasing with decreasing temperature or increasing probe size, and a weak component at long times with a rather erratic behaviour. Earlier studies<sup>3,17-20</sup> have convinced us that fitting four independent parameters in f.a.d. experiments was an aim at the limit of experimental possibilities. We believe that this is also true in the present study because the information contained in the noisy 'tail' of the experimental anisotropy is not sufficient to distinguish between, say, a 'long-time weak component' and a 'longer-time weaker' one. This is confirmed by the fact that, in most cases, the K expression which corresponds to an infinite-time second component leads to practically as good values of  $\chi^2$  as 2E. Finally, one must compare the amplitude of this infinite-time component ( $a_2 = r_{\text{inf}}$ ) with the finite accuracy of the baseline. This baseline is not perfectly well known, because of the uncertainties in the repositioning of polarizers, intensity fluctuations and a current-dependent background of the photomultiplier. This baseline was corrected using quinine sulphate, leading to a final accuracy no better than 0.005 to 0.01.

In the case of DPH, this is larger than the measured values of  $r_{\text{inf}}$  (which are also affected by uncertainties), so that no experimentally significant deviation from mono-exponential behaviour can be assessed (also compare Figures 1a and 1b). The situation for DPO is more ambiguous, since higher values of  $r_{\text{inf}}$  are obtained at low temperatures (typically  $r_{\text{inf}} = 0.05 \pm 0.02$ ), and the improvement of  $\chi^2$  between expression 1E and K is rather important. However, our present opinion is that these values of  $r_{\text{inf}}$  are still too poorly defined to ascertain the existence of a 'cage effect' for this probe in PBh. In any case, if such an effect exists it is very weak in the temperature range explored by f.a.d. (typically 100°C above  $T_g$ ). The question then arises of the difference between this conclusion and the more complex dynamics observed by Ouano and Pecora<sup>14</sup>. It is worth considering this previous experiment in some detail: these authors studied several mixtures of PMMA with chlorobenzene

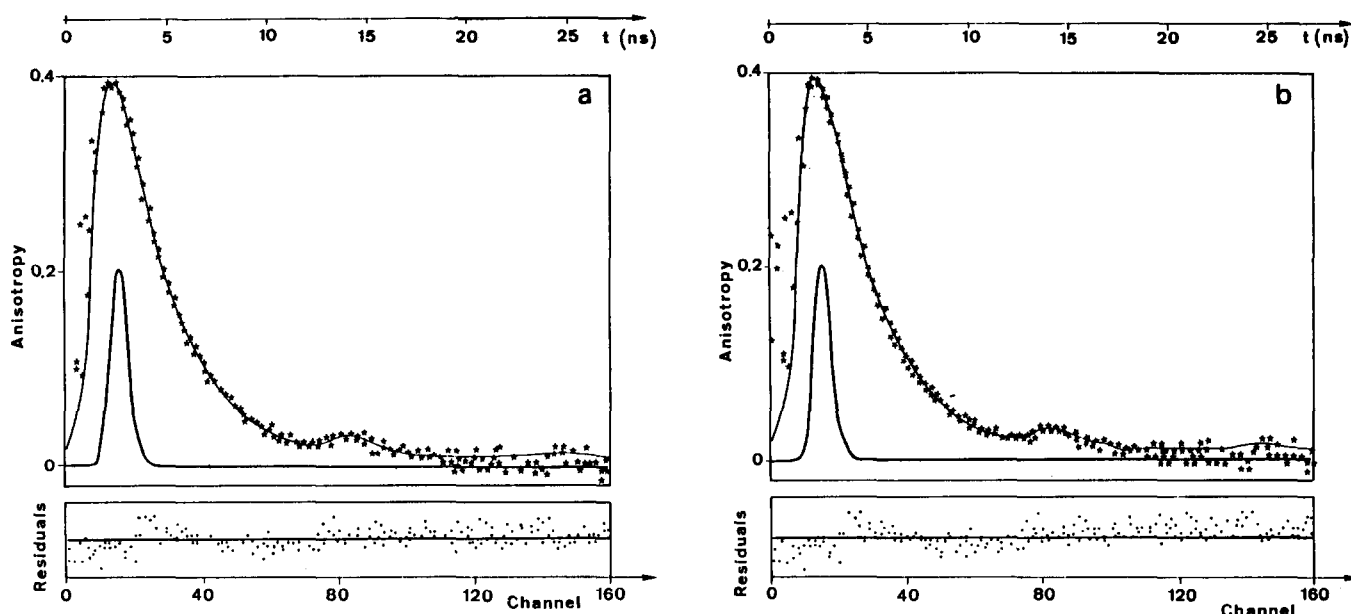


**Figure 1** Experimental f.a.d. (stars) and reconvoluted best fits for mono-exponential (a) and Kinosita (b) expressions, respectively. The weighted residuals are plotted in the lower frames

(CB) contents ranging from 20 to 80 wt%, in the temperature range 290–370 K. These conditions include systems both below and above  $T_g$ , but, in all cases, Ouano and Pecora observed two components with widely separated correlation times in the depolarized Rayleigh scattering. The ‘fast’ component is typically a few picoseconds, while the ‘slow’ one is in the nanosecond range, or slower (data at low CB concentration could not be resolved from the instrumental response). The relative amplitude of the ‘fast’ component regularly increased with temperature or CB content. Several interpretations of these results were proposed. The first one, called ‘restricted rotation diffusion’, associated the fast component to the rapid ‘free’ rotational diffusion of the CB in a cone that relaxes only slowly by cooperative polymer motions. The other interpretation was in terms of ‘diffusion in two environments’. In this approach, the CB can be either in a ‘fast’ or in a ‘slow’ environment, each environment leading to one of the components of depolarized Rayleigh scattering spectra.

Finally, Ouano and Pecora evoked the possibility that part of the CB molecules gather in ‘pools’ of higher mobility. It was not possible to choose between these different hypotheses. Indeed the interpretation of these depolarized Rayleigh scattering experiments is complicated by: (i) the multimolecular nature of the correlation functions; (ii) the high CB content, which makes the medium effectively two-component.

In contrast, our experiments involve a very low probe concentration, and directly probe the orientation autocorrelation function. They allow several definite conclusions:

(1) The essentially mono-exponential f.a.d. indicates that the rotation of a probe with simple geometry is essentially rotational diffusion, in the range explored (typically 100 ps  $\rightarrow$  100 ns).

(2) The value of  $r_0$  obtained in the fits,  $r_0=0.33$ , is rather close to the fundamental anisotropy of DPH in various or frozen media, which rules out an important extra picosecond component too fast to be resolved by our apparatus. Therefore no ‘cage effect’ or ‘restricted

rotation’ is observed for DPH in PBh about 100°C above  $T_g$ . Then it would be tempting to study the *OACF* of very dilute probes at lower temperatures to check if such effects occur closer to  $T_g$ .

Unfortunately, the millisecond–microsecond range is not available to fluorescence, and other highly sensitive methods available in this range, such as e.s.r.<sup>21</sup>, do not provide direct access to the *OACF*, making it difficult to understand the amplitude of the rotations observed. In the following, we leave this question in this rather incomplete state of understanding and we treat f.a.d. data using a model of isotropic rotation, valid within experimental error in the temperature range explored.

#### *Effect of probe size*

The theories of rotational diffusion provide definite predictions for the relationship between the dimensions of a molecule and the rotational correlation time. The early Stokes–Einstein model, restricted to spheres, has been extended to arbitrary ellipsoids with ‘sticking’ boundary conditions by Perrin<sup>22</sup>, and to ellipsoids with ‘slipping’ boundary conditions by Hu and Zwanzig<sup>23</sup>. Both models are hydrodynamic, in the sense that the molecule is represented by a rigid body embedded in a homogeneous viscous liquid. In the first case (stick), the fluid velocity tends towards the velocity of the body’s surface. In the second case (slip), only the component of the fluid velocity perpendicular to the surface of the body is correlated with the body’s surface velocity. This means that no void is created, but the fluid can ‘slip’ along the surface. On a molecular level, these models are supposed to represent two limiting cases in which: (i) the surrounding molecules closely follow the rotation of the probe (stick); (ii) the surrounding molecules rearrange to create the void necessary for the rotation of the probe, without following it (slip).

In principle the theories of Perrin and of Hu and Zwanzig are applicable to rigid molecules of any shape. However, only ellipsoids can be treated without heavy numerical work. Here we use a semi-quantitative approach, approximating DPH and DPO by spheroids.

The long and short hydrodynamic axes ( $L$  and  $I$  respectively), as calculated using the bond lengths and angles given by Pople and Gordon<sup>24</sup>, are:

$$\begin{aligned} L_{\text{DPH}} &= 18.3 \text{ \AA} & I_{\text{DPH}} &= 7.11 \text{ \AA} \\ L_{\text{DPO}} &= 20.7 \text{ \AA} & I_{\text{DPO}} &= 7.11 \text{ \AA} \end{aligned}$$

This corresponds to anisotropy ratios:

$$\rho_{\text{DPH}} = 2.58 \quad \rho_{\text{DPO}} = 2.91 \quad (4)$$

In using the Perrin formulac, the rotational diffusion coefficient of the long axis  $D_{\text{perp}}$  is related with  $\rho$ :

$$D_{\text{perp}} = \frac{3}{2}\rho \frac{[(2\rho^2 - 1)S - \rho]}{\rho^4 - 1} D \quad (5)$$

where

$$S = (\rho^2 - 1)^{-1/2} \log[\rho + (\rho^2 - 1)^{1/2}] \quad (6)$$

and  $D$  is the diffusion constant of a sphere with the same volume. Using relations (4) to (6), one predicts:

$$\left(\frac{\tau_{\text{DPH}}}{\tau_{\text{DPO}}}\right)_{\text{stick}} = \frac{D_{\text{DPO}}}{D_{\text{DPH}}} = \frac{0.444}{0.510} \frac{V_{\text{DPH}}}{V_{\text{DPO}}} = 0.77 \quad (7)$$

Using the values tabulated by Hu and Zwanzig, the ratio for slip boundary conditions should be:

$$\left(\frac{\tau_{\text{DPH}}}{\tau_{\text{DPO}}}\right)_{\text{slip}} = 0.63 \quad (8)$$

Comparison with the experimental values tabulated in Table 6 indicates that the friction conditions are close to 'slipping'. This behaviour, which is common in viscous non-associated fluids<sup>25</sup>, suggests that the probes are not strongly coupled with the polymer chains, but their motions should directly reflect the fluctuation of voids in the environment.

## EFFECT OF MOLECULAR WEIGHT AND TEMPERATURE

The effect of molecular weight on the dynamics of polybutadiene was investigated by combining further f.a.d. studies of the rotation of DPH in low-molecular-weight polybutadienes with d.s.c. experiments performed on the same samples, viscosity measurements, and excimer fluorescence (see part 1)<sup>1</sup>.

### Glass transition

The glass transition temperatures were obtained using a DuPont differential calorimeter (d.s.c.) operated at a heating rate of  $5^\circ\text{C min}^{-1}$ , and cyclohexane calibration. The plot of  $T_g$  versus  $1/M_n$  (Figure 2) is linear in agreement with the Fox-Flory expression, fruitfully applied to numerous polymer systems<sup>26-28</sup>:

$$T_g = T_g^\infty - A/M_n \quad (9)$$

**Table 6** Compared correlation times of DPH and DPO

$T$ (K)	315.6	304.5	293.9	280.8	269.5
$\tau_{\text{DPH}}$ (ns)	2.47	3.86	6.4	11.8	22.2
$\tau_{\text{DPO}}$ (ns)	3.99	6.39	11.9	23.5	42.0
$\tau_{\text{DPH}}/\tau_{\text{DPO}}$	0.62	0.60	0.54	0.50	0.53

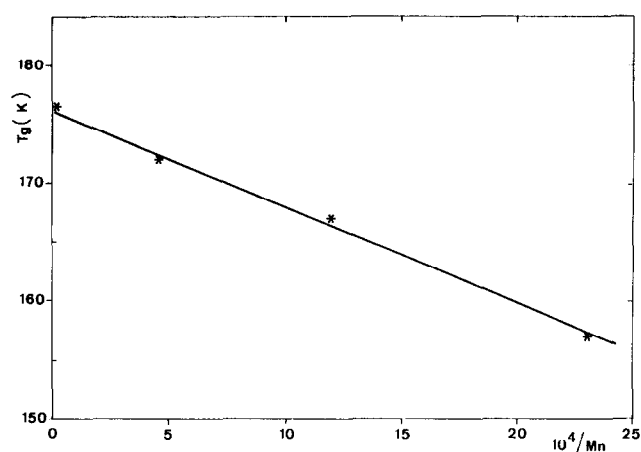


**Figure 2**  $T_g$  versus  $10^3/M_n$  (Fox-Flory plot) for PB

with parameters  $T_g^\infty = 176$  K and  $A = 9640$  g mol<sup>-1</sup>. This value of  $A$  fits well on the empirical curve proposed by Boyer<sup>28</sup>, together with that of other polymers with a low  $T_g$ . However, this result should be regarded with some caution, because, as discussed in part 1, the different polymers of the series also differ in their microstructure to some extent. The results for high-molecular-weight polybutadienes with different microstructures tabulated by Ferry indicate that the  $T_g$  and the WLF parameters depend weakly on the relative content of *cis* and *trans* concentration (Table 1), but that these parameters depend strongly on the vinyl content. Therefore, the good agreement with the Fox-Flory relationship obtained here may be somewhat fortuitous. Because of this complication, and of the limited number of molecular weights investigated, a more refined discussion using improvements of the original Fox-Flory expression, such as  $T_g = T_g^{\text{inf}} - A/(M + B)$ , and the corresponding interpretations<sup>28</sup>, seemed irrelevant here.

### Dynamics of DPH probes as a function of $M_n$

The dynamics of DPH in the series of low-molecular-weight polybutadienes was investigated in the range 228–328 K. As in the case of PBh, the f.a.d. is mono-exponential within experimental error, and the correlation time  $\tau$  regularly decreases with increasing temperature (Table 7). Figure 3 gathers the results as a function of  $10^3/T$ , showing curves linear and parallel within experimental error. The local activation energy is  $35 \pm 1$  kJ mol<sup>-1</sup> for all curves. As observed for  $T_g$ , the

**Table 7** Correlation times of DPH in low-molecular-weight matrices

PB500		PB1000		PB2500	
$T$ (K)	$\tau$ (ns)	$T$ (K)	$\tau$ (ns)	$T$ (K)	$\tau$ (ns)
226.7	51.9				
241.6	13.5	232.2	69.4	241.4	55.8
254.6	6.50	240.2	45.3	248.7	42.2
265.7	2.99	256.6	14.1	254.2	34.8
		271.8	5.68	265.9	17.4
278.8	1.48				
		284.7	2.68		
294.3	0.84	295.5	1.88	294.4	3.56
		305.1	1.48	304.8	2.14
				315.1	1.32

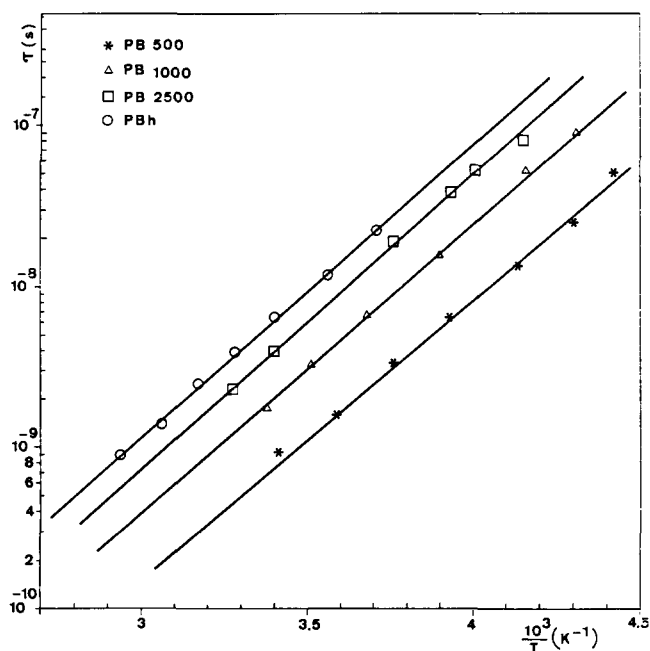


Figure 3 Correlation time of DPH in various PB matrices versus  $10^3/T$ : (○) PBh; (□) PB2500; (△) PB1000; (★) PB500

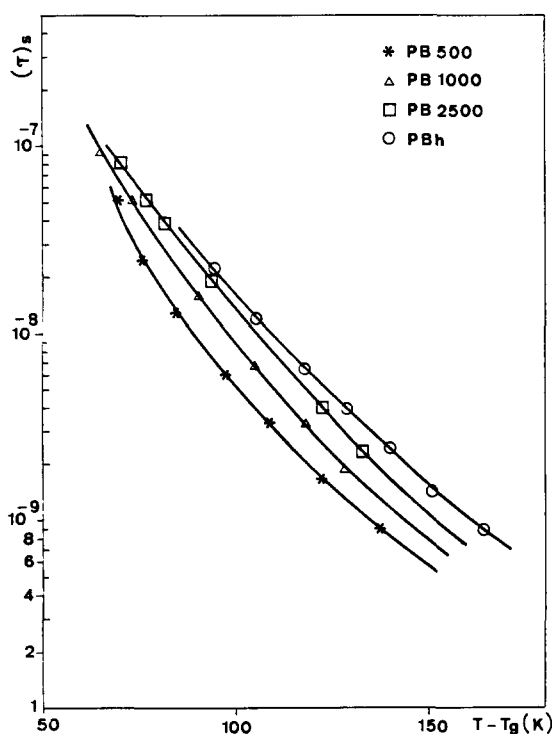


Figure 4 Correlation times of DPH versus  $T - T_g$  (symbols as in Figure 3)

correlation times seem to increase regularly with molecular weight, regardless of microstructure. However, a plot of  $\tau$  as a function of  $T - T_g$  (Figure 4) does not gather the results on a single master curve, as one would expect from a pure molecular-weight effect. It is generally admitted that only the  $T_g$  (or  $T_{inf}$ ) is affected by the molecular weight at first order<sup>29</sup>. However, the deviation is qualitatively consistent with the differences in microstructure quoted previously. The product of WLF parameters  $C_1 C_2$  for polybutadienes decreases with increasing vinyl content (see ref. 29 and Table 1).

Therefore the expansion coefficient of the free volume  $\alpha_f = 1/2.303 C_1 C_2$  increases with increasing vinyl content, and it is expected that PB500, which has the highest vinyl content, has the lowest correlation time at a given  $T - T_g$  (assuming that  $f_g$  is approximately constant).

We also attempted a direct determination of the WLF parameters. Writing the WLF equation in the general form<sup>1</sup>:

$$\frac{-1}{\log[\tau(T)/\tau(T_{ref})]} = \frac{1}{C_1^{ref}} + \frac{C_2^{ref}/C_1^{ref}}{(T - T_{ref})} \quad (10)$$

indicates that the plot of  $-1/\log[\tau(T)/\tau(T_{ref})]$  as a function of  $10^3/(T - T_{ref})$  should be linear for any value of  $T_{ref}$ . The coefficients  $C_2^{ref}/C_1^{ref}$  and  $1/C_1^{ref}$  correspond to the slope and the intercept, respectively. Using the arbitrary reference temperature,  $T_{ref} = 241.5$  K, we obtained the WLF parameters given in the last columns of Table 1. The results fall in a reasonable range for polybutadienes, and the evolution of the parameters with molecular weight and microstructure agree qualitatively with previous knowledge issued from viscoelasticity. However, a quantitative determination is unrealistic because our experimental window only involves a few decades of time, and because the experiments cannot be performed close to  $T_g$ . In a previous study of poly(propylene oxide)<sup>30</sup> we already noticed that the range of temperatures in which f.a.d. correlation times are measurable is too narrow and too far from  $T_g$  to allow an accurate determination of WLF parameters, if complementary spectroscopic measurements in a different temperature range, or an independent determination of  $T_{inf}$ , are not available. Such evaluations based on viscosity have been given in paper 1 for PB500 and PB1000. Using these values, (123 and 125 K, respectively) a plot of  $\log \tau_{DPH}$  as a function of  $10^3/(T - T_{inf})$  leads to estimates of the product  $C_1 C_2 = 451.5$  for PB500 and 487 for PB1000, respectively. As one would expect, these values are closer to those reported in part 1.

## CONCLUSIONS

We have considered two different aspects of local dynamics in polybutadiene. The first issue deals with the nature of the constraints exerted by the melt on the local motions, reflected here by the orientation autocorrelation function of rigid rod-like fluorescent probes. No decisive evidence for the 'cage effect' previously reported by Ouano and Pecora has been obtained in the temperature range available to the f.a.d. probe technique. We must restrict ourselves to a partial answer: if such a cage effect exists, it is weak, i.e. it concerns 10% residual orientation at most for DPO, and less for DPH. This means that the rotation is essentially a rotational diffusion, as it would be in ordinary viscous solvents. The 'viscoelastic' character of the melt is not apparent on the scale of 10–20 Å. This does not correspond to the observations of Ouano and Pecora, suggesting that, in these latter experiments, the multicomponent nature of the relaxation was due to the large concentration of chlorobenzene.

Comparing the correlation times of DPH and DPO, we reached the conclusion that the friction condition is of the 'slipping' type. Crudely speaking, this means that the probe moves by 'pushing away' surrounding molecules (or, equivalently, by occupying voids created by them).

This is in contrast with sticking boundary conditions, in which the probe and its close environment rotate together. The temperature dependence of the dynamics closely follows the WLF parameters deduced from viscoelastic data. This behaviour, which is often encountered in spectroscopic probe techniques (but not always), suggests that the probes (DPH and DPO) are large enough to require the fully developed cooperativity of the medium in order to perform its own motion. Using the model developed by Bullock *et al.*<sup>31</sup>, this corresponds to a probe factor close to 1, indicating that DPH is no smaller than the kinetic unit of the polybutadiene chains involved in the glass transition. Therefore, knowledge of the WLF coefficients completely defines the ratios of the correlation times of the probe at any temperature. The absolute value is imposed by a probe-dependent parameter  $\tau_0$ , defined by:

$$\log \tau_0 = \log \tau_c(T_g) - C_1^g \quad (11)$$

The values reported in *Table 1* are smaller than those obtained for meso-2,4-di(*N*-carbazolyl)pentane, which requires a larger volume for rearrangement, but the evolution from one matrix to the other is similar in the two techniques. Finally, the evolution of the dynamics with the molecular weight of the matrix is in agreement with the Fox-Flory model, but the situation is complicated by the different microstructures of the available samples of low molecular weight. The results are qualitatively consistent with the dependence of the WLF parameters upon the microstructure previously reported on the one hand, and with the Fox-Flory model on the other hand. Complementary experiments exploring a different time-temperature range would be necessary to reach a quantitative conclusion on this question.

#### ACKNOWLEDGEMENTS

We are indebted to L. Bokobza and D. Chassagnard for fruitful discussions, and for assistance in the microstructure determination.

#### REFERENCES

- 1 Bokobza, L., Pham-Van-Cang, C., Monnerie, L., Vandendriessche, J. and de Schryver, F. C. *Polymer* 1989, **30**, 45

- 2 Dale, R. E. in 'Time-Resolved Fluorescence Spectroscopy in Biochemistry and Biology' (Eds. R. B. Cundall and R. E. Dale) NATO-ASI Series, Vol. 69, Plenum Press, New York, 1983
- 3 Viovy, J. L., Monnerie, L. and Merola, F. *Macromolecules* 1985, **18**, 1130
- 4 Wahl, P. *Biophys. Chem.* 1979, **10**, 91
- 5 Brochon, J. C. in 'Protein Dynamics and Energy Transduction' (Ed. Shin'ichi Ishiwata), Taniguchi Foundation, Japan, 1980
- 6 Valeur, B. and Monnerie, L. *J. Polym. Sci., Polym. Phys. Edn.* 1976, **14**, 11
- 7 Birks, J. B. and Birch, D. J. S. *Chem. Phys. Lett.* 1975, **31**, 608
- 8 Cehelnik, E. D., Cundall, R. B., Lockwood, J. R. and Palmer, T. F. *J. Phys. Chem.* 1975, **79**, 1369
- 9 Birch, D. J. S. and Imhof, R. E. *J. Phys. E: Sci. Instrum.* 1977, **45**, 1044
- 10 Wahl, P., Auchet, J. C. and Donzel, B. *Rev. Sci. Instrum.* 1974, **45**, 28
- 11 Bouchy, M., Jezequel, J. Y., Andre, J. C. and Bordet, J. in 'Deconvolution and Reconvolution of Analytical Signals' (Ed. M. Bouchy), Nancy, Proceedings, 22 July, ENSIC-INPL Editions, France, 1982
- 12 Dale, R. E., Chen, L. A. and Brand, L. *J. Biol. Chem.* 1977, **252**, 7500
- 13 Kawato, S., Kisosita, K. and Ikegami, A. *Biochemistry* 1977, **16**, 2163
- 14 Ouano, A. C. and Pecora, R. *Macromolecules* 1980, **13**, 1167
- 15 Kinosita, K., Kawato, S. and Ikegami, A. *Biophys. J.* 1977, **20**, 289
- 16 Tao, T. *Biopolymers* 1969, **8**, 609
- 17 Viovy, J. L., Monnerie, L. and Brochon, J. C. *Macromolecules* 1983, **16**, 1845
- 18 Viovy, J. L. *J. Phys. Chem.* 1985, **89**, 5465
- 19 Viovy, J. L. and Monnerie, L. *Adv. Polym. Sci.* 1985, **67**, 99
- 20 Barkle, M. D., Kowalczyk, A. A. and Brand, L. *J. Chem. Phys.* 1981, **75**, 3581
- 21 Tormala, P. *J. Macromol. Sci.-Rev. Macromol. Chem. (C)* 1979, **17** (2), 297
- 22 Perrin, F. *J. Phys. Radium* 1934, **5**, 497; *ibid.* 1936, **7**, 1
- 23 Hu, C. H. and Zwanzig, Z. *J. Chem. Phys.* 1974, **60**, 4354
- 24 Pople, J. A. and Gordon, M. J. *Am. Chem. Soc.* 1967, **89**, 4253
- 25 Alms, G. R., Bauer, D. R., Brauman, J. I. and Pecora, R. *J. Chem. Phys.* 1973, **58**, 3570; *ibid.* 1973, **59**, 5310; *ibid.* 1973, **59**, 5321
- 26 Fox, T. G. and Flory, P. J. *J. Am. Chem. Soc.* 1948, **70**, 2384; *J. Appl. Phys.* 1950, **21**, 581; *J. Polym. Sci.* 1954, **14**, 315; *J. Phys. Chem.* 1951, **55**, 221
- 27 Fox, T. G. and Losaheh, S. *J. Polym. Sci.* 1955, **15**, 371
- 28 Boyer, R. F. *Macromolecules* 1974, **7**, 142
- 29 Ferry, J. D. 'Viscoelastic Properties of Polymers', 3rd Edn., Wiley, New York, 1980
- 30 Fofana, M., Veissier, V., Viovy, J. L., Monnerie, L. and Johari, G. P. *Polymer* 1988, **29**, 245
- 31 Bullock, A. T., Cameron, G. G. and Miles, I. S. *Polymer* 1982, **23**, 1536; *ibid.* 1986, **27**, 190